Phenomenological study of the $pp \to \pi^+ pn$ reaction

G. Fäldt[1,*] and C. Wilkin[2,†]
[1]*Department of Physics and Astronomy, Uppsala University, Box 516, 751 20 Uppsala, Sweden*
[2]*Physics and Astronomy Department, UCL, Gower Street, London WC1E 6BT, United Kingdom*

(Received 21 October 2017; published 13 February 2018)

Fully constrained bubble chamber data on the $pp \to \pi^+ pn$ and $pp \to \pi^+ d$ reactions are used to investigate the ratio of the counting rates for the two processes as function of the pn excitation energy Q. Though it is important to include effects associated with the p-wave nature of pion production, the data are insufficient to establish unambiguously the dependence on Q. The angular distributions show the presence of higher partial waves which seem to be anomalously large at small Q. The dispersion relation method to determine scattering lengths is extended to encompass cases where, as for the $pp \to \pi^+ pn$ reaction, there is a bound state and, in a test example, it is shown that the values deduced for the low-energy neutron-proton scattering parameters are significantly influenced by the pion p-wave behavior.

DOI: 10.1103/PhysRevC.97.025201

I. INTRODUCTION

The most complete measurements of the $pp \to \pi^+ pn$ differential cross section were carried out using the Petersburg Nuclear Physics Institute (PNPI) bubble chamber exposed to proton beams with kinetic energies between 900 and 1000 MeV [1–3]. The measured and deduced four-vectors of the final particles for all the events at the three energies studied are available on the Bonn-Gatchina website [4]. Although it was shown that much of the data could be described through the excitation of the $\Delta(1232)$ isobar through pion exchange [1–3], it is of interest to see what features could be explained using less prescriptive model approaches.

The final-state interaction (FSI) theorem [5] links the production of S-wave spin-triplet pn pairs in the $pp \to \pi^+ pn$ reaction to the cross section for $pp \to \pi^+ d$. The failure of the theorem to describe the bubble chamber data was ascribed to the production of higher partial waves in the recoiling proton-neutron system at even low pn excitation energy Q [6]. By studying the ratio of the $pp \to \pi^+ pn$ and $pp \to \pi^+ d$ cross sections as a function of Q, as well as the angular distribution of the produced pn pairs, it is shown in Sec. II that the behavior for $Q < 20$ MeV is anomalous, possibly due to the strong tensor force that couples the S and D waves. Though the p-wave nature of pion production has to be taken into account when evaluating the predictions, this does not affect the basic conclusions.

Though it is hard with the present data to isolate the contribution from higher partial waves just on the basis of the FSI theorem, we turn in Sec. III to the question of whether $pp \to \pi^+ pn$ could in principle be used to investigate the properties of the low-energy pn system. Though data on $pp \to K^+ \Lambda p$ have been directly fitted to determine the Λp scattering length [7], an alternative approach has been advocated that uses a dispersion relation in an approximate treatment that only requires data over a limited range in Q [8–10]. In the derivation of this formalism, it is assumed that there is no true bound-state pole and in Sec. III we generalize this method to treat the $pp \to \pi^+ pn$ reaction, where the final pn pair could combine to produce a true bound state, namely the deuteron. By considering the predictions of a simplified model, the predicted pn parameters are studied as functions of the cutoff in the dispersion relation description with and without considering the p-wave nature of pion production. In analogy to our analysis of the $pp \to K^+ \Lambda p$ reaction [11], it is shown that it is the position of the nearby pole in the pn channel that remains completely stable and the scattering length itself is much more model dependent.

Our conclusions are to be found in Sec. IV.

II. COMPARISON OF THE $pp \to \pi^+ pn$ AND $pp \to \pi^+ d$ PRODUCTION RATES

The final-state interaction theorem relates the normalizations of the wave functions for S-wave bound and scattering states [5]. This has been exploited to predict the double-differential center-of-mass (c.m.) cross section for the S-wave spin-triplet component in $pp \to \pi^+ pn$ in terms of the cross section for $pp \to \pi^+ d$ [12]:

$$\frac{d^2\sigma}{d\Omega\, dx}(pp \to \pi^+ \{pn\}_t) = F(x)\, \frac{p_\pi(x)}{p_\pi(-1)}\, \frac{\sqrt{x}}{2\pi(x+1)}\, \frac{d\sigma}{d\Omega}(pp \to \pi^+ d). \quad (1)$$

Here x denotes the excitation energy Q in the np system in units of the deuteron binding energy B_t, $x = Q/B_t$, and $p_\pi(x)$ and $p_\pi(-1)$ are the pion c.m. momenta for the pn continuum and deuteron, respectively. In a single-channel situation, the normalization $F(x = -1) = 1$ at the deuteron pole but it was

*goran.faldt@physics.uu.se
†c.wilkin@ucl.ac.uk

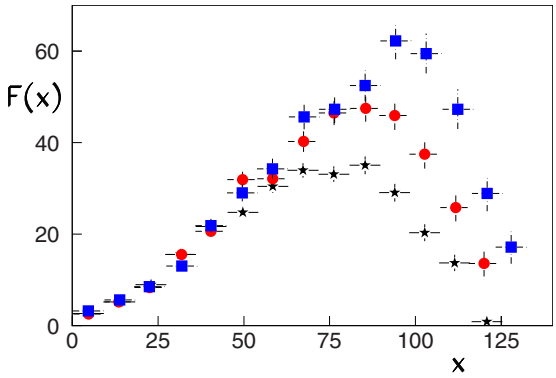

FIG. 1. Values of $F(x)$ extracted from the PNPI bubble chamber data at 900.2 MeV [1] (black stars), 940.7 MeV [2] (red circles), and 988.6 MeV [3] (blue squares) using Eq. (1), The errors shown do not include those arising from the numbers of $pp \to d\pi^+$ events measured since these affect all the data at a given beam energy. The laboratory beam energies quoted here are the nominal ones listed in Refs. [1–3].

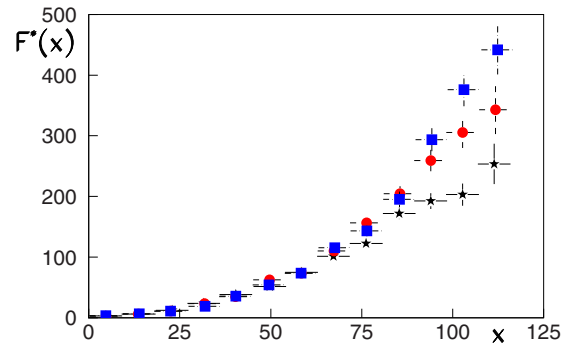

FIG. 2. Values of $F^*(x)$ extracted from the PNPI bubble chamber data at 900.2 MeV [1] (black stars), 940.7 MeV [2] (red circles), and 988.6 MeV [3] (blue squares) on the basis of Eqs. (1) and (2). The errors shown do not include those arising from the numbers of $pp \to d\pi^+$ events measured. Deviations between the values of $F^*(x)$ for different energies at large x are due in part to the spread in the measured beam energy; the nominal beam energies are used in the evaluation of the momentum factor of Eq. (2).

argued [5] that deviations from this value should be small at low x if the pion production operator is of short range and the tensor force linking the S and D states in the deuteron could be neglected. However, although the shape of the high-resolution inclusive data at 951 MeV, where only the π^+ was measured [13], is plausibly described by Eq. (1) up to an excitation energy of $Q \approx 20$ MeV, reproducing the average absolute magnitude for $x \lesssim 9$ requires $F(x) = 2.2 \pm 0.1$. It should here be noted that the contribution from S-wave spin-singlet np pairs was shown to be very small at 951 MeV [13].

Using bubble chamber data on single-pion production in proton-proton collisions at three energies between 900 to 1000 MeV [1–3], it is clear that the excess of $F(x)$ over unity for low Q is primarily due to higher partial waves in the final proton-neutron system [6]. This conclusion was based upon a study of the angular distribution of the pn relative momentum in the rest frame of the two nucleons. It is thus important to see if extra information could be obtained through a study of the dependence of the data on the excitation energy in the pn system.

Figure 1 shows the values of $F(x)$ extracted from the PNPI bubble chamber data at three beam energies [1–3] using Eq. (1). Although we are mainly interested in the behavior at small Q, it is clear from the figure that there remains a significant dependence on the beam energy, though the overall errors arising from the small numbers of measured $pp \to d\pi^+$ events have not been included. In particular, the data at large x show an effect that seems to be linked to the finite phase space. The effect is not caused by approximations in Eq. (1) regarding the phase space limits but rather it is due to the fact that the reaction is dominated by the excitation of the $\Delta(1232)$, which necessarily involves a p-wave pion and hence a pion momentum factor in the production amplitude. The pion momentum vanishes at the kinematic limit of large x and this feature leads to the maxima seen in Fig. 1. It is therefore more appropriate to consider

$$F^*(x) = \left[\frac{p_\pi(-1)}{p_\pi(x)}\right]^2 F(x), \tag{2}$$

which takes the p-wave nature of the pion production into account. Note, however, that $F^*(x = -1) = F(x = -1)$ so that the extrapolation to the deuteron pole is unaffected by the modification introduced through Eq. (2).

The variation of $F^*(x)$ with x is illustrated in Fig. 2. The modification introduced through Eq, (2) removes the maxima seen in Fig. 1 and the data increase up to the largest value of x allowed by the kinematics. Of crucial importance is the fact that the data at different beam energies now overlap much better so that $F^*(x)$ is a more universal observable. Deviations from "universality" at large x are due in part to the spread in the measured beam energy, which is particularly significant in the 900 MeV data [1]. It should be noted that the nominal beam energies are used in the evaluation of Eq. (2).

The $F^*(x)$ data of Fig. 2 were fit in the range $20 < Q < 180$ MeV to the quadratic form

$$F^*(x) = A + B(x+1) + C(x+1)^2 \tag{3}$$

where, according to the FSI theorem [5], the value of the parameter A should be unity. Given the wide range of $F^*(x)$ shown in the figure, it is not surprising that this value was not confirmed by the data; free fits give $A = 3.3 \pm 1.6$, 9.0 ± 2.0, and 12.0 ± 2.3 at the three energies. The error bars should be treated with some caution because the values obtained for A change significantly if higher order polynomials are used in the fit.

Imposing the constraint $A = 1$ on the average of the three data sets shown in Fig. 3 leads to a reasonable description of the data for $20 < Q < 180$ MeV with $B = -0.054 \pm 0.026$ and $C = 0.0223 \pm 0.0007$. The data at larger values of x clearly require a higher order polynomial to achieve an acceptable description. Thus, it is clear that the $Q > 20$ MeV data are not inconsistent with the FSI prediction of $A = 1$ but, in view

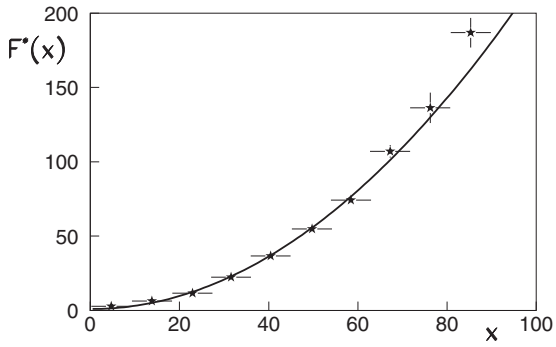

FIG. 3. Values of $F^*(x)$ averaged over the PNPI beam energies of 900.2, 940.7, and 988.6 MeV [1–3] obtained using Eqs. (1) and (2). The curves are fits made on the basis of Eq. (3) with $A = 1$ (fixed), $B = -0.054$, and $C = 0.0223$.

of the limited statistics, they cannot provide any supporting evidence.

The principal drawback in using Eq. (1) is that it only leads to estimates of the cross section where the final proton-neutron pair in the $pp \to pn\pi^+$ reaction is in a relative S state. A very useful tool for investigating the effects of higher pn waves was developed by Gottfried and Jackson [14]. They defined an angle θ_p, which is that between the final proton and the incident beam direction in the pn rest frame. Any deviation from isotropy in this angle is unambiguous evidence for the production of higher partial waves in the final pn system.

It was already pointed out [6] that, even for $Q < 20$ MeV, the distributions of the bubble chamber events [1–3] were not isotropic. In order to increase the statistics, in Fig. 4 the events at all three beam energies are combined and these show how the anisotropy grows from $Q \sim 10$ to $Q \sim 150$ MeV. It should be noted that since the protons in the initial state are identical, the distribution must be symmetric about 90° so that the experimental data have been folded about this point.

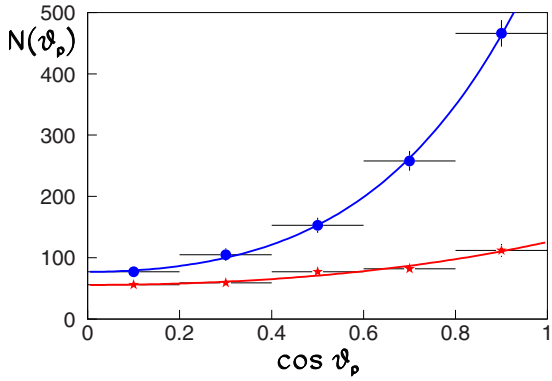

FIG. 4. Distributions in the Gottfried-Jackson angle θ_p for all the $pp \to pn\pi^+$ PNPI bubble chamber events in the range 900–1000 MeV [1–3]. The (red) stars correspond to data chosen with $0 < Q < 20$ MeV, whereas the (blue) circles are those where $140 < Q < 160$ MeV. The lines represent the Legendre polynomial curves of Eq. (4), with the values of the fitted parameters C_2 and C_4 being shown in Fig. 5.

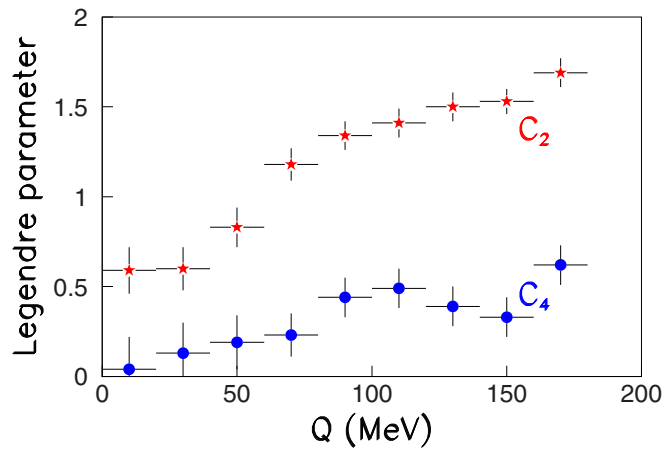

FIG. 5. Variation of the parameters C_2 (red stars) and C_4 (blue circles) of the Legendre polynomial fit of Eq. (4) to the Gottfried-Jackson angular distribution observed in the PNPI bubble chamber measurements of the $pp \to pn\pi^+$ differential cross section [1–3].

The distributions in the θ_p angle were fitted with the Legendre polynomial expansion

$$N(\theta) = C_0[1 + C_2 P_2(\cos\theta) + C_4 P_4(\cos\theta)] \qquad (4)$$

and the values of the parameters C_2 and C_4 thus obtained are plotted in Fig. 5 for the different energy bins. The resulting curves and data are also shown at two energies in Fig. 4.

Any nonvanishing of the C_2 or C_4 parameter would be an indication of higher partial waves in the np system but, since it is impossible from these data to distinguish the squares of P waves from S-D interference, one can at best only establish weak lower bounds on any such contribution. On general grounds, one expects that close to threshold the C_2 parameter should vary like Q and C_4 like Q^2. The obvious deviation from this rule seen in Fig. 5 is in the value of C_2 in the lowest Q bin, which shows that higher pn partial waves are important for Q even below 20 MeV [6], and this might be connected with the strong tensor force in the spin-triplet pn system.

III. DETERMINING THE NEUTRON-PROTON SCATTERING PARAMETERS FROM THE $pp \to pn\pi^+$ REACTION

The Q dependence of the $pp \to pn\pi^+$ cross section is sensitive to the low-energy pn scattering parameters and a similar sensitivity is expected in the $pp \to \Lambda pK^+$ reaction provided that the Λp system emerges in a relative S wave. The angular distribution shown in Fig. 4 proves that this is not a valid assumption for $Q < 20$ MeV in the $pp \to pn\pi^+$ case [6] and there are similar doubts for $pp \to \Lambda pK^+$ when $Q < 40$ MeV [15].

Even if we could identify the Λp S-wave contribution in say the $pp \to \Lambda pK^+$ reaction, there are still difficulties in extracting the Λp scattering length due, in part, to the finite range of Λp invariant masses accessible and the coupling to the inelastic channels, as well as to the limited mass resolution. An alternative approach has been advocated that exploits the analyticity of the amplitudes through the use of a dispersion

relation [8,9]. It was shown that estimates of the S-wave Λp phase shift can be deduced from the $pp \to \Lambda p K^+$ data through

$$\frac{\delta(k)}{k} = -\frac{1}{2\pi}\sqrt{\frac{m_{\rm min}}{m_{\rm red}}}\int_{m_{\rm min}^2}^{m_{\rm max}^2} d\mu^2 \sqrt{\frac{m_{\rm max}^2 - {m_X}^2}{m_{\rm max}^2 - \mu^2}} \times \frac{1}{\sqrt{\mu^2 - m_{\rm min}^2}\,(\mu^2 - {m_X}^2)} \log\left\{\frac{A(\mu)}{A(m_X)}\right\}, \quad (5)$$

where the principal value integral in the original derivation has been here replaced by a standard Riemann integral [11].

In the above, k is the relative momentum in the Λp system and $m_{\rm red}$ is the corresponding reduced mass so that, nonrelativistically, $Q = k^2/2m_{\rm red}c^2$. $A(\mu)$ is the enhancement factor of the $pp \to \Lambda p K^+$ cross section with respect to phase space as a function of the Λp invariant mass μ. If one only takes the Λp final-state interaction into account then $A \propto |J(k)|^{-2}$, where $J(k)$ is the Λp Jost function. The lower limit of the integration is $m_{\rm min} = m_p + m_\Lambda$ and the Λp mass is fixed by the external kinematics as $m_X = m_{\rm min} + Q/c^2$. Ideally, the upper integration limit $m_{\rm max}$ should be taken to be infinite but in general this is not practical because of the desire to retain only the S wave in the Λp system. The authors of Refs. [8,9] therefore made the approximation of cutting the integration at $Q = Q_{\rm max}$, which they chose to be $Q_{\rm max} = 40$ MeV. In this way, they could obtain estimates for the Λp scattering length and effective range, though at the expense of introducing a theoretical uncertainty associated with the cutoff energy.

Even if the contribution from higher partial waves, for which there is some evidence from the Gottfried-Jackson distribution [15], is discounted, it has been shown [11] that Eq. (5) leads to a much better determination of the position of the virtual pole in the Λp system than it does of the scattering length or effective range individually. We now want to apply the methodology to the $pp \to pn\pi^+$ reaction.

Apart from the increased complications due to the pion multiple scatterings, the critical difference between the $pp \to \Lambda p K^+$ and $pp \to pn\pi^+$ reactions is that there is a true bound state, the deuteron, in the pn system whereas the virtual state pole in the Λp case is on the second sheet. The derivation of Eq.(5) must therefore be modified accordingly and this can be accomplished following Eq. (12.63) of Newton's book [16]. Suppose that there is just one bound state at $k = i\alpha$. In the *reduced* S-wave Jost function the bound-state pole is replaced by one corresponding to a virtual state, $\alpha \to -\alpha$, by constructing

$$J^{\rm red}(k) = J(k)\left(\frac{k + i\alpha}{k - i\alpha}\right). \quad (6)$$

For real k, the magnitudes of the two Jost functions are identical:

$$|J^{\rm red}(k)| = |J(k)|. \quad (7)$$

Since the phase of the Jost function is determined by the S-wave phase shift δ,

$$J(k) = |J(k)|\exp(-i\delta), \quad (8)$$

it follows immediately that the reduced phase shift is related to the true one through

$$\delta^{\rm red}(k) = \delta(k) - i\log\left(\frac{k + i\alpha}{k - i\alpha}\right). \quad (9)$$

For small values of k, $i\log[(k + i\alpha)/(k - i\alpha)] \approx -\pi + k/\alpha - k^3/3\alpha^3$. The $-\pi$ term, which is a consequence of Levinson's theorem when there is one bound state, does not contribute in the evaluation of $\cot\delta$. It can therefore be neglected so that, effectively, for small k,

$$\delta(k) = \delta^{\rm red}(k) + 2k/\alpha - 2k^3/3\alpha^3 + O(k^5), \quad (10)$$

where it is $\delta^{\rm red}(k)$ that is approximated by the formulas of Ref. [8], with a virtual rather than a bound state.

In a low-energy expansion, the S-wave phase shift can expressed in terms of the scattering length a and effective range r as

$$\delta(k) = -ka + a^2k^3(a/3 - r/2) + O(k^5). \quad (11)$$

Using this expansion in Eq. (10) for both $\delta(k)$ and $\delta^{\rm red}(k)$, and comparing terms of order k and k^3, shows that

$$a_1 = a_0 - 2/\alpha,$$
$$a_1^2(a_1 - 3r_1/2) = a_0^2(a_0 - 3r_0/2) - 2/\alpha^3, \quad (12)$$

where a_1 and r_1 are the scattering length and effective range when the pole is a bound state and a_0 and r_0 are the corresponding parameters when there is a virtual bound state at $k = -i\alpha$.

It must be emphasized that apart from the change in the sign of α, the parameters of the true and reduced Jost functions are identical, though this is by no means obvious when looking at the very different values of the scattering length and effective range determined by Eq. (12).

It would, of course, be preferable to test the methodology described above on experimental data but, as shown by the Gottfried-Jackson distributions [14], higher partial waves contribute in $pp \to pn\pi^+$ at even small values of Q [6]. We use instead data generated from the one-pole Jost function, where

$$J(k) = \frac{k - i\alpha}{k + i\beta}. \quad (13)$$

This form corresponds to the Bargmann potential where the expressions for the scattering length and effective range are, respectively,

$$a = \frac{\alpha + \beta}{\alpha\beta} \quad \text{and} \quad r = \frac{2}{\alpha + \beta}. \quad (14)$$

Although the exact numbers are not crucial for the purposes of a test, the experimental spin-triplet values of $a = 5.414$ fm and $r = 1.757$ fm [17] correspond to parameters $\alpha = 0.2315$ fm^{-1} and $\beta = 0.9055$ fm^{-1} for the Bargmann potential.

Estimates of a_0 and r_0 were made on the basis of the dispersion integral of Eq. (5) using the Jost function of Eq. (13) with the sign of α changed so that there is a virtual rather than a true bound state. The corresponding bound state case was then treated by employing the relations given in Eq. (12). The results are shown in Fig. 6 as functions of $Q_{\rm max}$. In order to be consistent with the potential description, nonrelativistic

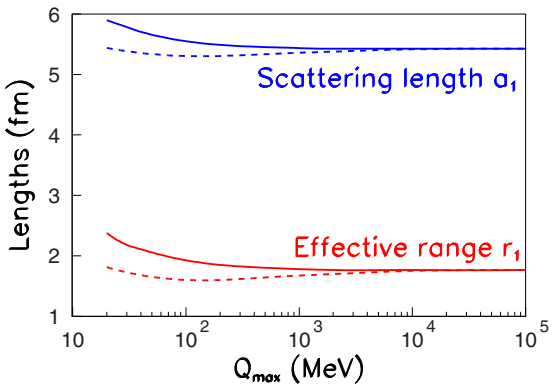

FIG. 6. Estimates of the spin-triplet np scattering length (a_1) and effective range (r_1) deduced from Eqs. (5) and (12) as functions of the cutoff energy $Q_{\max}$ in the integration. The true values with no cutoff should be $a_1 = 5.414$ fm and $r_1 = 1.757$ fm. The solid lines were obtained with the *bare* Jost function of Eq. (13) as input but with $\alpha \to -\alpha$. The dashed lines were derived by using the modified Jost input of Eq. (15), where the effects of the p-wave nature of the pion production have been included.

kinematics have been used in the studies, even though this is hard to justify for $Q_{\max} \gtrsim 100$ MeV.

It must be noted that the pole position α_0 determined from Eq. (5) should be identical to that of the input because this is determined uniquely by the singularity in $A(m_X)$, which is independent of the value of $Q_{\max}$. It then follows from Eq. (9) that the pole position of the bound state, α_1, should be equally stable to changes in the value of $Q_{\max}$. However, for small $Q_{\max}$, where higher order terms in the effective range expansion become relatively more important, it is necessary to take these into account when extracting the value of α.

The variation of the np scattering length a_1 with the integration cutoff parameter $Q_{\max}$ is less strong than in our previous work on the $pp \to K^+\Lambda p$ reaction [11]. This can be linked to the different value of β/α since Eq. (14) shows that for large β the scattering length is fixed primarily by the value of α, which is very stable. These arguments do not, of course, apply to the effective range r_1.

It was remarked already in the papers on the dispersion integral approach to the analysis of $pp \to K^+\Lambda p$ data [8–10] that the value obtained for the Λp scattering length could be distorted through a reflection of the production of N^* isobars in the $K^+\Lambda$ channel. This is typically a problem of limited energy where the Dalitz plot is not sufficiently open and the dependence on the three invariant masses cannot be independently determined. We saw in the description of the bubble chamber data on $pp \to \pi^+ pn$ [1–3] in Fig. 2 that it was important to take the p-wave nature of the $\Delta(1232)$ into account and so it is interesting to study the estimates made in the dispersion relation approach using as input an enhancement factor of the form

$$A = \left(\frac{k^2+\beta^2}{k^2+\alpha^2}\right)(p_\pi)^2\,, \tag{15}$$

where the pion momentum p_π is a function of x and hence of k^2.

The effect of the pion momentum factor depends on the limits of phase space and, at very high energies, p_π is essentially constant over the relevant part of the integration in Eq. (5), in which case the results would be indistinguishable from those obtained using the *bare* Jost function. For the purposes of the test, we have assumed that the available energy is twice that of the cutoff energy $Q_{\max}$. The resulting estimates for the scattering length and effective range are compared in Fig. 6 with the predictions of a_1 and r_1 obtained without the pion momentum factor.

Just as for the *bare* Jost input, within numerical uncertainties the position of the virtual state pole remains stable at $\alpha_0 = -0.2135\,\text{fm}^{-1}$ and $\alpha_1 = -\alpha_0$. On the other hand, if one derives values of the parameter β from Eq. (14), it is seen that these are identical for the virtual and true bound state cases, i.e., $\beta_1 = \beta_0$, and that β approaches the input value for large $Q_{\max}$. In general, though, the value of β obtained in the pion p-wave case is bigger than that for the *bare* Jost input because it effectively reduces the strength at larger k^2.

IV. CONCLUSIONS

Using the PNPI bubble chamber data, we have investigated two features of the $pp \to \pi^+ pn$ reaction in ways that minimize the model dependence. Though we had earlier shown that the cross section at low-np excitation energy Q was high as compared to that of $pp \to \pi^+ d$, and that this was probably linked to the production of higher partial waves in the np system [6], studies of the cross section ratio presented here do not clarify sufficiently the effect. However, the deviations from the predictions of the final-state interaction theorem [5,12] are particularly large in the lowest Q bin. This might arise from the strong tensor force in the np system. This discrepancy is little affected by the distortions induced by the production of the $\Delta(1232)$ isobar.

Even though the behavior of the $pp \to \pi^+ pn/pp \to \pi^+ d$ ratio with Q could not be investigated completely with the limited statistics of the bubble chamber experiments, it is of interest to ask to what extent such data could in principle be used to investigate the neutron-proton scattering length. We generalized the dispersion relation approach of Refs. [8,9] to situations where, as in this case, there is a true bound state in the np system. The results of this, or a direct-fitting approach to the data, are influenced by the dominantly p-wave nature of pion production and, if this is not taken into account, a systematic error is made in the extracted value of the np scattering length.

Although the value obtained for the scattering length changes with the cutoff, or whether the pion p-wave factor is included or not, the position of the bound-state pole remains completely fixed, so that it is primarily this parameter that could be fixed by the data rather than the scattering length and effective range separately. This parallels our discussion of the $pp \to K^+\Lambda p$ reaction, where it is the position of the virtual bound state that could be determined by good data [11]. All this assumes, of course, that data can be obtained with purely S-wave np or Λp events. As is clear from Fig. 4, this presents more of a challenge as Q is increased, which reinforces our argument that the data should be used to fix the pole rather

than the scattering length. This will remain true even if the pion multiple scatterings are taken into account, though these will undoubtedly complicate the extrapolation to the deuteron pole.

ACKNOWLEDGMENTS

We are grateful to Dr. Hauenstein for providing us with the distribution in the Gottfried-Jackson angle for the $pp \to K^+\Lambda p$ reaction for $Q < 40$ MeV.

[1] K. N. Ermakov, V. I. Medvedev, V. A. Nikonov, O. V. Rogachevsky, A. V. Sarantsev, V. V. Sarantsev, and S. G. Sherman, Eur. Phys. J. A **50**, 98 (2014).

[2] K. N. Ermakov, V. I. Medvedev, V. A. Nikonov, O. V. Rogachevsky, A. V. Sarantsev, V. V. Sarantsev, and S. G. Sherman, Eur. Phys. J. A **47**, 159 (2011).

[3] K. N. Ermakov, V. A. Nikonov, O. V. Rogachevsky, A. V. Sarantsev, V. V. Sarantsev, and S. G. Sherman, Eur. Phys. J. A **53**, 122 (2017).

[4] Bonn-Gatchina Partial Wave Analysis [pwa.hiskp.uni-bonn.de]

[5] G. Fäldt and C. Wilkin, Phys. Scr. **56**, 566 (1997).

[6] G. Fäldt and C. Wilkin, Phys. Lett. B **770**, 146 (2017).

[7] A. Budzanowski, A. Chatterjee, H. Clement, E. Dorochkevitch, P. Hawranek, F. Hinterberger, R. Jahn, R. Joosten, K. Kilian, S. Kliczewski *et al.* (HIRES Collaboration), Phys. Lett. B **687**, 31 (2010).

[8] A. Gasparyan, J. Haidenbauer, C. Hanhart, and J. Speth, Phys. Rev. C **69**, 034006 (2004).

[9] A. Gasparyan, J. Haidenbauer, and C. Hanhart, Phys. Rev. C **72**, 034006 (2005).

[10] F. Hauenstein, E. Borodina, H. Clement, E. Doroshkevich, R. Dzhygadlo, K. Ehrhardt, W. Eyrich, W. Gast, A. Gillitzer, D. Grzonka *et al.* (COSY-TOF Collaboration), Phys. Rev. C **95**, 034001 (2017).

[11] G. Fäldt and C. Wilkin, Phys. Rev. C **95**, 024004 (2017).

[12] A. Boudard, G. Fäldt, and C. Wilkin, Phys. Lett. B **389**, 440 (1996).

[13] M. Abdel-Bary, A. Budzanowski, A. Chatterjee, J. Ernst, P. Hawranek, F. Hinterberger, V. Jha, K. Kilian, S. Kliczewski, D. Kirillov *et al.* (GEM Collaboration), Phys. Lett. B **610**, 31 (2005).

[14] K. Gottfried and J. D. Jackson, Nuovo Cimento **33**, 309 (1964).

[15] F. Hauenstein (private communication).

[16] R. G. Newton, *Scattering Theory of Waves and Particles* (Springer-Verlag, New York, 1982).

[17] O. Dumbrajs, R. Koch, H. Pilkuhn, G. C. Oades, H. Behrens, J. J. de Swart, and P. Kroll, Nucl. Phys. B **216**, 277 (1983).